An exploration of the effectiveness of artificial mini-magnetospheres as a potential solar storm shelter for long term human space missions

R.A. Bamford [a,*], B. Kellett [a], J. Bradford [a], T.N. Todd [b], M.G. Benton Sr.[c], R. Stafford-Allen [b], E.P. Alves [d], L. Silva [d], C. Collingwood [a], I.A. Crawford [e], R. Bingham [f,a]

[a] RAL Space, STFC, Rutherford Appleton Laboratory, Harwell Oxford, Didcot OX11 0QX, UK
[b] Culham Centre for Fusion Energy, Culham Science Centre, Abingdon, Oxfordshire OX14 3DB, UK
[c] The Boeing Company, El Segundo, CA 90009-2919, USA
[d] GoLP/Instituto de Plasmas e Fusão Nuclear, Instituto Superior Técnico, 1049-001 Lisboa, Portugal
[e] Department of Earth and Planetary Sciences, Birkbeck College, London
[f] University of Strathclyde, Glasgow, Scotland, UK

ABSTRACT

If mankind is to explore the solar system beyond the confines of our Earth and Moon the problem of radiation protection must be addressed. Galactic cosmic rays and highly variable energetic solar particles are an ever-present hazard in interplanetary space.

Electric and/or magnetic fields have been suggested as deflection shields in the past, but these treated space as an empty vacuum. In fact it is not empty. Space contains a plasma known as the solar wind; a constant flow of protons and electrons coming from the Sun.

In this paper we explore the effectiveness of a "mini-magnetosphere" acting as a radiation protection shield. We explicitly include the plasma physics necessary to account for the solar wind and its induced effects. We show that, by capturing/containing this plasma, we enhance the effectiveness of the shield. Further evidence to support our conclusions can be obtained from studying naturally occurring "mini-magnetospheres" on the Moon. These magnetic anomalies (related to "lunar swirls") exhibit many of the effects seen in laboratory experiments and computer simulations. If shown to be feasible, this technology could become the gateway to manned exploration of interplanetary space.

1. Introduction

The World's space agencies are actively planning for human space missions beyond Low Earth Orbit [1], and the scientific benefits resulting from human exploration of the Moon, Mars and asteroids are likely to be considerable [2–4].

However, the risk posed by radiation beyond Earth's magnetosphere is one of the greatest obstacles to long term human space exploration [31,5,6]. Thus careful consideration must be given to radiation protection.

The US National Research Council Committee on the Evaluation of Radiation Shielding for Space Exploration [6] recently stated:

"Materials used as shielding serve no purpose except to provide their atomic and nuclear constituents as targets to interact with the incident radiation projectiles, and so

* Corresponding author.
E-mail address: ruth.bamford@stfc.ac.uk (R.A. Bamford).
URL: http://www.minimagnetospheres.org (R.A. Bamford).

either remove them from the radiation stream to which individuals are exposed or change the particles' characteristics – energy, charge, and mass – in ways that reduce their damaging effects."

This paper outlines one possible way to achieve this, by radically reducing the numbers of particles reaching the spacecraft. The technology concerns the use of "Active" or electromagnetic shielding – far from a new idea (for reviews see [34,12]) – but one which, until now, has been analysed without considering some crucial factors, leading to an expectation of excessive power requirements.

The missing component is a self-consistent analysis of the role played by the plasma environment of interplanetary space.

Presented here are the answers to three questions:

(1) What difference is made by the fact that the interplanetary space environment contains a low density (approximately 10 per cm^{-3}) plasma of positive and negative charges, to how a potential artificial electromagnetic radiation shield would work on a manned spacecraft?
(2) How differently does a plasma behave at the small scales of a spacecraft compared to, say, the magnetosphere barrier of a planet?
(3) How does this change the task of balancing the cost and benefits of countermeasures for engineers designing an interplanetary or long duration manned mission?

Initiatives such as *Earth–Moon–Mars Radiation Environment Module (EMMREM)* [11] aim to provide frameworks to overcome the mission safety challenges from Solar Energetic Particles (SEP).[1] Accurate prediction of space "storms" is only valuable however if the means exist to protect the spacecraft and its crew.

In this paper we discuss the principles and optimisation of miniature magnetospheres. The upper panel in Fig. 1 shows a photograph of a mini-magnetosphere formed in the laboratory [21] in an experiment based on the theory outlined here. Furthermore, these principles have now been borne out by observation and analysis of naturally occurring mini-magnetospheres on the Moon [39,40]. The theory provides a self-consistent explanation for the manifestation of "Lunar swirls" [19].

The lower panel in Fig. 1 illustrates a mini-magnetosphere around a conceptual manned interplanetary spacecraft.

1.1. Mini-magnetospheres and plasmas

In space the charged particles (protons, electrons and other trace ions) mostly originate from the sun. A *magnetosphere* is a particular type of "diamagnetic cavity" formed within the *plasma* of the solar wind.

Plasma is a state of matter in which the diffuse conglomeration of approximately equal numbers of positive and negative charges are sufficiently hot that they do not recombine significantly to become neutral particles. Rather the charges remain in a dynamic state of quasi-neutrality,

interacting, and self-organising in a fashion which depends upon the interaction of internal and external electromagnetic forces. These are the attributes to be exploited here as a means to protect vulnerable manned spacecraft/planetary bases.

In interplanetary space the high energy component of the solar particles forms the "hazard" itself, in particular because of the high penetrating capability of energetic ions. These are the Solar Cosmic Rays (SCR). A smaller percentage (about 6 orders of magnitude less) of super energetic particles at GeV energies have been accelerated by exotic events such as super-novas. These form the Galactic Cosmic Ray (GCR) component. Both high fluxes of SCR during storms and the long term exposure to GCR are a threat to astronaut health [10].

Space plasmas are very diffuse indeed, with about 10 particles occupying the volume of the end of the average human thumb, and are considered ultra high vacuum by terrestrial standards. The mean-free-path between physical collisions between the particles is far longer than the system (in solar wind the mean-free-path is about 1 A.U., Astronomical Unit). This means the particles "collide" through their electrostatic charges and collective movements (such as currents) which are guided by, or result in, magnetic or electric fields.

Because of the large dimensions of space, even a very low density is important. The electrostatic forces between two charges are 10^{39} times more intense than their gravitational attraction [13].

A plasma is a rapidly responding conducting medium due to the free moving charges. It creates a magnetic field in opposition to an externally applied magnetic field, making it diamagnetic, and can result in local cavities. Diamagnetic cavities are a general phenomenon in plasmas, not only in space plasmas, and can be formed with or without magnetic fields [41].

Magnetospheres are more generally associated with planetary magnetic fields (such as that of the Earth) interacting with the solar wind plasma [15]. Miniature magnetospheres are fully formed magnetospheres, with collisionless shocks and diamagnetic cavities, but the whole structure is very much smaller, of the order of 110-100 s of km across. Mini-magnetospheres have been observed associated with the anomalous patches of surface magnetic field which exist on the Moon [16], Mars [18] and Mercury [20], and also with asteroids such as Gaspra and Ida [17]. It has also been demonstrated that mini-magnetospheres can form without the presence of magnetic fields. Examples include natural comets [23] and artificial comets such as AMPTE [24]. In these cases the term "magneto" can still be used because the currents induced in the sheath region include magnetic fields. Mini-magnetospheres are determined by the plasma physics of the very small scale which in general has been neglected in the analysis of the electromagnetic deflection as a means of spacecraft protection. The entire structures are smaller than the bending radius of an energetic ion about the magnetic field in a vacuum. Therefore this is not a conventional "magnetic shield".

Presented here is a "block diagram" of the characteristics and parameters needed to implement a mini-magnetosphere deflector shield for a manned space craft.

---

[1] SEPs are sometimes called Solar Particle Events (SPE) also, the term "Proton" is occasionally substituted for "Particle".
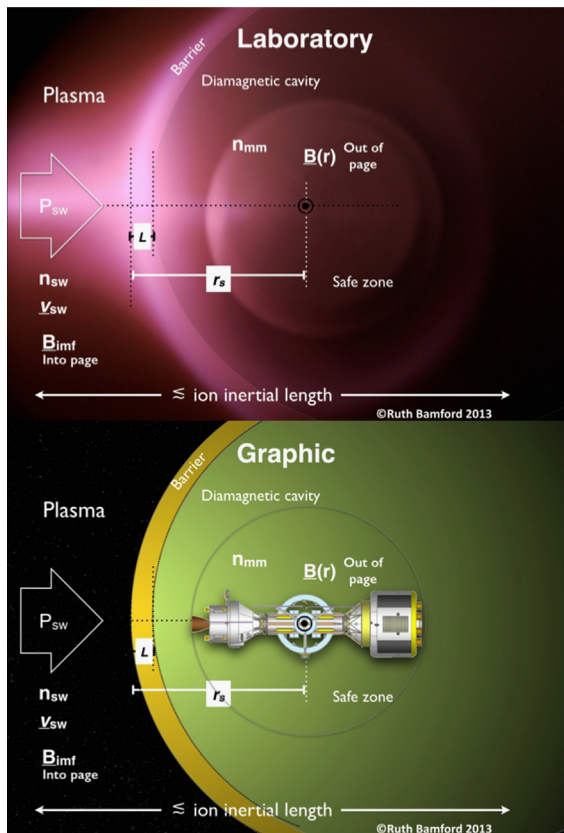
Fig. 1. A magnetically held plasma barrier creating an artificial mini-magnetosphere in the laboratory [21] (upper panel) and conceptually around a spacecraft (lower panel). Above: The supersonic hydrogen plasma (pink glow) from the Solar Wind Tunnel is flowing from the left and encounters a magnetic field (inside the protective casing visible in the photograph). The self-captured plasma forms a thin sheath barrier which diverts the incoming hazard. A cavity in the density is created within, confirmed by probe measurements [21]. This photograph is taken from above looking through the sheath onto the south pole. The graphic below shows the various zones whose characteristics are discussed in this paper and their relationship to a conceptual spacecraft [22]. Importantly in the laboratory experiment the overall dimensions are of the order, or less than that, of the ion skin depth c/ω_{pi} which must essentially be of practical size. The width L of the current sheath is approximately the electron skin depth $L \sim c/\omega_{pe}$. The pressure balance between incoming and defensive forces occurs at distance $\mathbf{r}_s$ from the source of the magnetic field. Together these parameters define the effectiveness of the active shield. (Conceptual spacecraft design © Mark Benton, Sr.). (For interpretation of the references to colour in this figure caption, the reader is referred to the web version of this paper.)

The actual physics of the interaction is immensely complex and largely non-deterministic analytically due to non-linearities. Thus these are "rules of thumb", intended only as a guide. A fully detailed analysis will require the use of complex plasma physics and simulation codes. Due to the resources needed this would best be conducted on a specific case for which as much verifiable data as possible is available.

2. The hazard

At the radius of the Earth's orbit the level of ultra-violet radiation from the Sun is sufficiently high that photo-ionisation results in almost all matter in free space being ionised. The medium of space is therefore a plasma, albeit of very low density. Solar eruptions consist of electromagnetic waves but also protons and electrons with a small percentage of higher mass ions.

The radiation encountered in space (see Fig. 2) is a composite of a small percentage of extremely high-energy galactic particles and a higher density but, much lower energy continuous outflow of particles from the sun (the solar wind), interspersed with intermittent, high density eruptions of very energetic particles originating from a variety of violent events on the sun. Events on or near the sun which result in shockwaves can accelerate ions and electrons to extremely high energies [28,29]. An example showing the temporal and energy spectra of large Solar Energetic Particle (SEP) events is shown in Fig. 3 [30].

One of the more recent large Solar Energetic Particle (SEP) events illustrates the magnitude of the problem [30]. The temporal plot of particle flux from [30] is shown in Fig. 3(a). The x-ray flare on the Sun provided only a few minutes' warning before high-energy > 0.5 GeV protons arrived at Earth, peaking within 5 min. Approximately 10 min later, the peak in the > 100 MeV protons arrived. At its peak the particle flux rate was $\sim \times 10,000$ the background level. A second peak occurred about 90 min later and, over the next 12 h, directional, lower energy particles continued to arrive, still at unusually raised densities.

For a spacecraft in interplanetary space, such an event produces intense bursts of radiation of deeply penetrating particles capable of passing through the hull to the crew within. The result is a significant and dangerous increase in dose-rates above 0.05 Gy/h [32].

The variable shape of the energy spectrum for each SEP is an extremely important factor for the total exposure calculation and not just the total fluence. For instance, protons with energies above 30 MeV can pass through space suits, while those above 70–100 MeV can pass
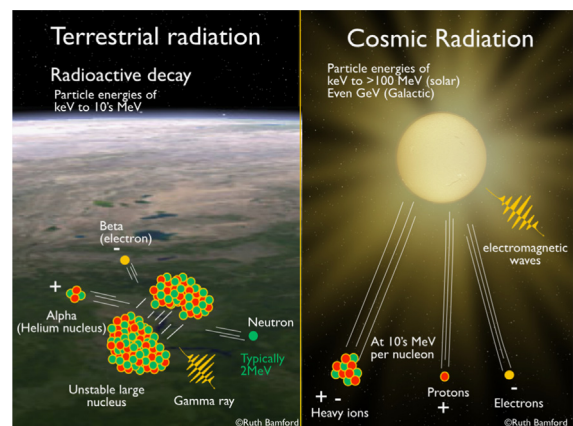

Fig. 2. A different type of "radiation" in space. Radiation hazard on Earth is generally related to radioactive decay of heavy elements like uranium and electromagnetic waves like gamma and x-rays (left). The radiation in space has a broadband electromagnetic component and also has an additional form of radiation not seen on Earth except in particle accelerators and as cosmic rays. Extreme forces in the centres of galaxies and supernova explosions can accelerate protons, alpha particles, and heavy nuclei, such as iron, to energies from MeV to 100's of GeV. At these energies the particles are predominantly the nuclei of atoms and electrons separately constituting a high energy plasma.
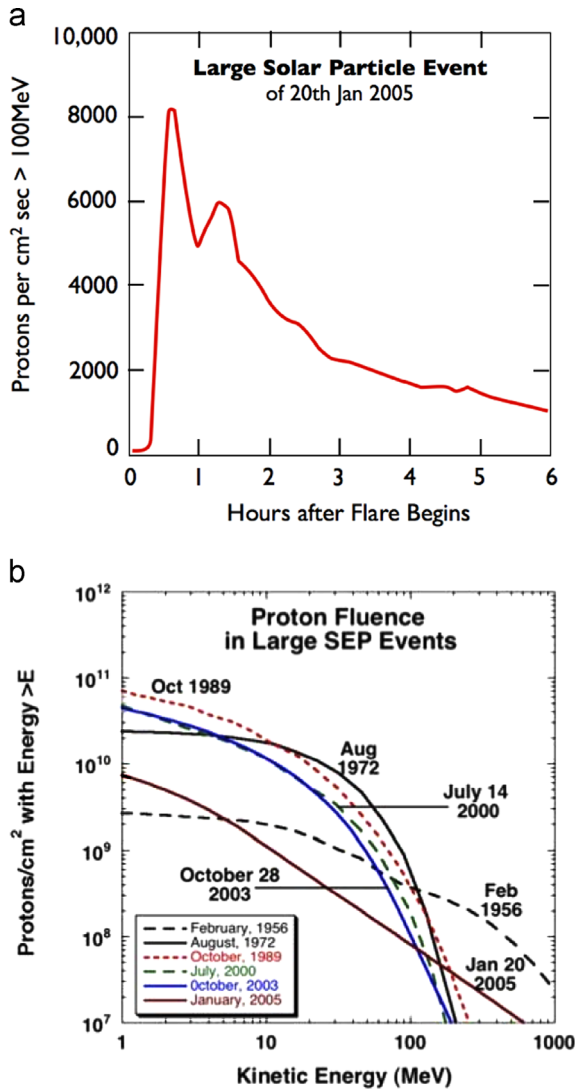
a

b

Fig. 3. (a) The time evolution of proton fluence for a large storm. High-energy > 0.5 GeV protons arrived at Earth, peaking within 5 min followed 10 min later by the peak > 100 MeV fluence, $\sim \times 10,000$ the background level. Over the next 12 h directional, lower energy particles arrived, still at raised densities. (b) The energy fluence spectra of some of the largest SEP events of the last 50 years [30]. Under normal conditions the numbers of particles with energies > 10 MeV are negligible. But increases of 10–1000 times during an SEP are typical and can rise to as much as 10^6 for more extreme events [30].

through aluminium spacecraft hull walls of 5–10 g cm^{-2}, with the added consequences of secondary particle radiation. The energy spectrum of some of the largest events (based on fluence of particles) of the last 50 years is shown in Fig. 3(b) [30].

The vulnerability of different organs and systems (such as blood forming organs or nervous system) varies considerably [7,9,33]. Thus it becomes difficult to quantify the potential mission disruption caused by solar events based purely on predicted severity of the event.

Current estimates [8] suggest that there is $\sim 20\%$ chance of exceeding the current NASA 30-day limit for a future SEP with $\Phi_{30} = 2 \times 10^9$ protons cm^{-2} during an

interplanetary journey. The probability of multiple events increases with mission duration.

For long term interplanetary manned missions, protection against extremely large SEP which occur sporadically and with very little warning is a mission critical issue [31,5].

2.1. Particle description of the incoming pressure

The characteristics of the instantaneous plasma (quasi-neutral collection of approximately equal numbers of positive and negative charges), particle distributions impacting the spacecraft, define how the plasma shield will function at any one instant.

The pressure from the environmental plasma P_{in} can consist of more than one component. Considering a thermal part, bulk flow ram pressure and pressure from the magnetic field in the solar wind:

$$P_{in} = P_{th,sw} + P_{ram,sw} + P_{B_{IMF}} + P_{ram,++} \qquad (2.1)$$

The component terms being $P_{th} = n_{th}kT_{th}$, $P_{ram} = n_{sw}m_{sw}\mathbf{v}_{sw}^2$ and $P_{B_{IMF}} = |\mathbf{B}_{IMF}^2|/2\mu_o$. Here n_{sw} represents the density of particles flowing at velocity $\mathbf{v}_{sw}$ and $\mathbf{B}_{IMF}$ is the Interplanetary Magnetic Field (IMF). The final term is the ram pressure from the high energy particles $P_{ram,++}$ which has been differentiated from the main distribution for this analysis. As can be seen from Fig. 3(b) the density of particles at the high energy tail can be a significant fraction of the bulk density but in general can be considered a negligible fraction of the total pressure.

As will be seen below, although variable, the background "solar wind" plasma is what is used initially to *create the barrier*, it can be artificially augmented to increase the deflection of the hazardous high energy component of the particle spectrum.

3. Mini-magnetospheres

3.1. Pressure balance

The principle of "Active Shielding" requires electromagnetic forces to balance the incoming pressure. (Many authors have reviewed the general principles of Active Shielding, for example [34]).

We start with a generic expression of the required pressure balance:

$$P_{mm} = P_{th,mm} + P_{ram,mm} + P_{B_{mm}} \qquad (3.1)$$

Here the subscripts represent the pressures from within the mini-magnetosphere. The ram component, although it exists due to the motion of the spacecraft, is merely a frame of reference issue and effectively insignificant. In many cases the thermal outward pressure is also insignificant. So, to first order, a magnetosphere pressure balance provides:

$$P_{B_{mm}} \approx P_{ram,sw}. \qquad (3.2)$$

As will be shown, an electric field is generated by the formation of a mini-magnetosphere, so this term will remain. If we create an artificial mini-magnetosphere on board the spacecraft we can define the initial $P_{B_{mm}}$.

4. Creating an artificial mini-magnetosphere

An on-board "Mini-Mag" system would most likely consist of a superconducting coil [36].

In a non-conductive medium, the magnetic field intensity of a dipole magnetic field diminishes rapidly with range. Higher-order structures, such as quadrapoles and octopoles, have fields which decrease more rapidly with radius from the coils which create them.

Fig. 4 shows the magnetic field at a distance (in the "far-field") where $r \gg a$ (in any direction) is $|B_{vac}(r)| \approx |B_o(a/r)|^3$ but only when no plasma is present. Or in terms of the current in the coil:

$$B(r) \approx \left(\frac{\mu_o I}{2a}\right)\left(\frac{a}{r}\right)^3 \qquad (4.1)$$

Here I is the total loop-current of the solenoid $I = NI_c$, where N is the total number of turns carrying current I_c at radius of a.

The presence of the plasma changes the profile. This can be seen illustrated in Fig. 5.

The prohibitively high power estimates of a magnetic shield are based on the vacuum profile (the near field plot generation and profile with distance is shown in Fig. 4). The vacuum field power estimates do not allow for the alteration in the profile and additional force illustrated in Fig. 5.

The effect of the plasma environment is not just to extend the range of the magnetic field intensity. The effect of the magnetic "pile-up" comes with cross field currents in a narrow barrier region (or shell in 3D) some distance from the spacecraft. These currents and accompanying electric fields alter the way in which the incoming plasma is deflected. The efficiency of the shielding is therefore found to be much greater than the initial vacuum calculation would have predicted. Evidence that this is the case will be shown in Section 7.
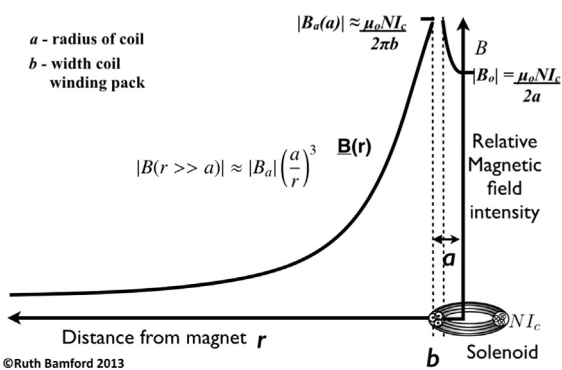

Fig. 4. How the vacuum magnetic field intensity varies with range from the spacecraft based on solenoid characteristics. The magnetic field of a flat round coil of major radius$=a$, with N turns of current carrying windings of I_c the current in each turn results in a total amp-turns of $I = NI_c$ and provides a magnetic field intensity at the centre of the coil of B_o. The highest magnetic field is $B_o(b)$ and is at the surface of the winding pack where b is the minor radius of the winding pack. As can be seen from the figure the magnetic field intensity in the centre can be less than that at the outer edge of the winding pack. The wider the radius the more this is the case, and the greater the range of the field beyond the spacecraft. With a central magnet (or multipole magnets) the magnetic field intensity will diminish more rapidly than for a wide diameter loop.
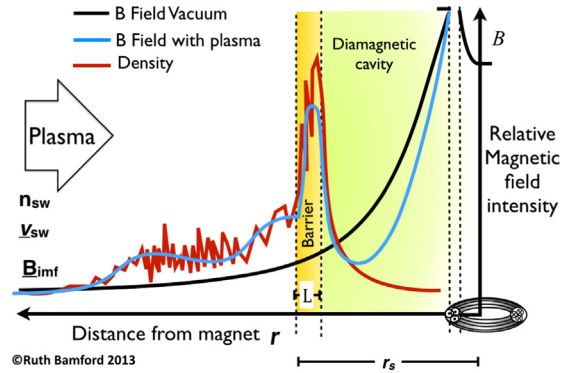

Fig. 5. A plot illustrating the difference in magnetic field made by the plasma environment. The "foot region" is caused by ion reflection and is of the order of the ion inertial length whereas the current or barrier layer width, L, is associated with the electron inertial length. Ideally $r_s \geq L$. Because the interaction is a collisionless-shock, the initial pile-up of density and magnetic field is accompanied by turbulence and a reduction in the velocity of the ions as well as changes in temperature of both the ions and electrons. Inside the barrier region is the cavity where the population of energetic particles is reduced. For optimum efficiency this need only to be sufficiently wide to afford the required degree of protection.

Quantifying the level of enhancement and the effectiveness at deflecting higher energy particles is non-trivial. In the following section we shall provide estimates which can be used to determine the value of an artificial mini-magnetosphere shield for astronaut protection.

5. Characterising the effectiveness of an artificial mini-magnetosphere

Fig. 1 shows a two dimensional sketch of the morphology of a mini-magnetosphere surrounding a spacecraft. The size of the mini-magnetosphere is dependant upon two parameters.

Firstly, r_s the "stagnation" or "stand-off" distance of a magnetopause is where the pressure of the incoming plasma, P_{in}, is balanced by the combined pressure of the mini-magnetosphere.

The second parameter is L the width of the magnetopause boundary. Clearly, to be within the safety of a mini-magnetosphere diamagnetic cavity, one must be further away than the thickness of the boundary.

In kinetic studies of mini-magnetospheres we find that $L \approx$ electron skin depth.

5.1. Calculating stand-off distance, r_s

To first order, Eq. (2.1), the magnetosphere pressure can be taken to be approximately balanced by the vacuum magnetic field: $P_{in} \approx P_B$. However, as can be seen in Fig. 5, something interesting happens when the opposing forces approach balance. The magnetic field profile deviates radically from the vacuum profile, as it is now determined by the plasma. Precisely how, is described by plasma kinetic effects (also referred to as finite Larmor radius effects).

This balance occurs at a distance r_s from the source of the magnetic field. In planetary magnetospheres r_s would be the Chapman–Ferraro distance. The same calculation for an artificial source provides an estimate of the relationship

between on-board power requirements and shield effect-iveness.

For a dipole magnetic field produced by a solenoid, such as that shown in Fig. 4, the magnetic field at the centre of the solenoid $B_o = \mu_o N I_c / 2a$, where a is the radius of the solenoid loop containing total loop turns of $I = N I_c$ (N, number of turns; I_c, current per turn). This provides:

$$r_s^6 \sim \frac{\mu_o (N I_c)^2}{8 P_{in}} a^4 \qquad (5.1)$$

Here P_{in} is obtained from Eq. (2.1). This same calculation for the Earth's magnetosphere leads to a consistent under-estimation of the true stand-off distance indicating the importance of the other terms in Eqs. (2.1) and (3.1).

Interestingly Eq. (5.1) reveals that the largest possible stand-off distance is achieved with the largest possible coil radius. This is intuitively reasonable because the long-range field strength diminishes with B_{oa}^3, so a small change in the radius of the coil has a large effect, far more so than the peak field in the centre of the coil.

5.2. Calculating barrier width, L

The plasma physics of the interaction [41,42] tells us that the width of the magnetopause boundary L is of the order of the electron skin depth λ_e:

$$L \approx \lambda_e = \frac{c}{\omega_{pe}} \qquad (5.2)$$

Here ω_{pe} is the electron plasma frequency, $\omega_{pe} = (n_e e^2 / \epsilon_o m_e)^{1/2}$, c is the speed of light.

The classical skin depth is a rapid decay of electro-magnetic fields with depth inside a conductor caused by eddy currents in the conductor. High frequencies and high conductivity shorten the skin depth as does an increase in the number of current carriers (plasma density).

The same is true here with some differences. For instance, the conditions of a collisionless shock of the mini-magnetosphere mean that the attenuation profile is closer to a linear approximation profile than the $1/e$ attenuation in metals.

5.3. The normalised linear attenuation factor, α

We can now introduce a geometric parameter α as a *quasi*-linear attenuation factor. This is to provide an indication of relative effectiveness.

The number of skin depths required for complete ambient plasma exclusion is not generally known but values of 4–6 have been calculated up to relativistic energies [43]. This is similar to the exponential[2] form of the electromagnetic skin depth in metals. However, given the level of other approximations being made in these formulations, we shall take a normalised parameter where the number of required skin depths is taken to be =1:

$$\alpha := \frac{r_s}{L} \qquad (5.3)$$

---

[2] The plasma physics here provides a more linear rather than exponential drop off.

The plasma for this calculation can be a combination of the incoming plasma density and any additional density added from the spacecraft to enhance the shield effectiveness.

The assumed value of $r_s = L$ is good, $r_s > L$ would be better if multiple skin depths $r_s \sim 4$–$6 \times L$, and $r_s < L$ is less than optimum.

5.4. The origin of the electric field

The expressions above provide an estimation of how the bulk pressures balance. For a practical shield to reduce the penetrating high energy component we need to determine the value of the electric field within the barrier – and how it can effect the exclusion of higher energy particles. Fig. 6 is a close up view of Fig. 1 with the force vectors overlaid. The particle trajectory of a representative high energy ion velocity $\mathbf{v}_{++}$ and mass M is also shown.

The forces on the charged particle are determined by the Lorentz force:

$$\mathbf{F} = q(\mathbf{E} + \mathbf{v} \times \mathbf{B}). \qquad (5.4)$$

Unlike in a vacuum, the presence of the plasma means that $\mathbf{E}$ cannot be neglected and is related to $\mathbf{B}$.

The electric field component comes from the formation of currents which are induced to exclude the interplane-tary magnetic field and create the cavity.

The physics of collisionless shocks provides us with an expression for the instantaneous electric potential compo-nent, ϕ, responsible for slowing and deflecting the ions such that:

$$\phi(r) \approx -\frac{\kappa}{n_{mm}} \frac{|\Delta B_{mm}|^2}{\Delta r} \qquad (5.5)$$

Here κ is a constant $\kappa = 1/(2\mu_0 e)$. If $|\Delta B_{mm}| \sim |B_{mm}|$ is the intensity of the magnetic field orthogonal to $\mathbf{r}$ and $\mathbf{v}$ at distance $(r_s - L)$, then $\Delta r \sim L$.

Eq. (5.5) shows that the potential is related to the *gradient* in the magnetic field intensity, or the *ponderomo-tive force*. This is a much more effective and short-range force than calculations of the magnetic bending alone would suggest. Because the density within the mini-magnetosphere, n_{mm}, is within both κ and L (from Eq. (5.2)), the magnitude of $\phi \propto \sqrt{n_{mm}}$. This offers a means to boost the effectiveness of the deflector shield by adding additional density. This will be discussed in Section 5.6.

5.5. High energy particle deflection

The electric field created is responsible for changing the energy and trajectory of the energetic particles.

Although the electric field values from Eq. (5.5), with augmented plasma density, will not be sufficient to stop a > 100 MeV or GeV ion, this is not necessary. The particles need only be *refracted* sufficiently away from the central safe-zone. Much like tackling a charging football player, rather than stand in his way to protect the goal line, a better policy is to *deflect* the player sideways using a small amount of force so that he is pushed "into touch" and out of the field of play.
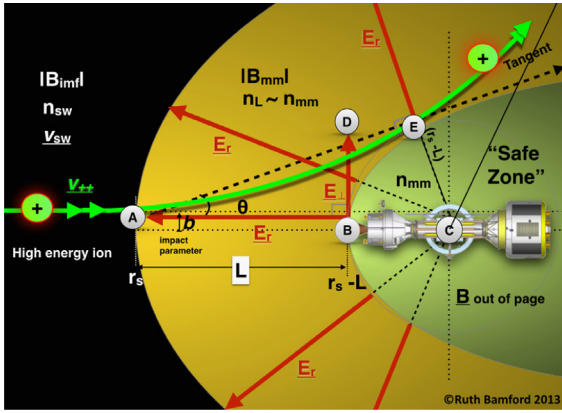
Fig. 6. The deflection of a high energy ion (green) by the electric field (E_r) (red) created by the low energy plasma captured and retained by the magnetic field from the spacecraft. Augmenting the natural density, by releasing readily ionised gas from the craft, can enable protection of ⩾ 100 MeV/amu ions. (For interpretation of the references to colour in this figure caption, the reader is referred to the web version of this paper.)
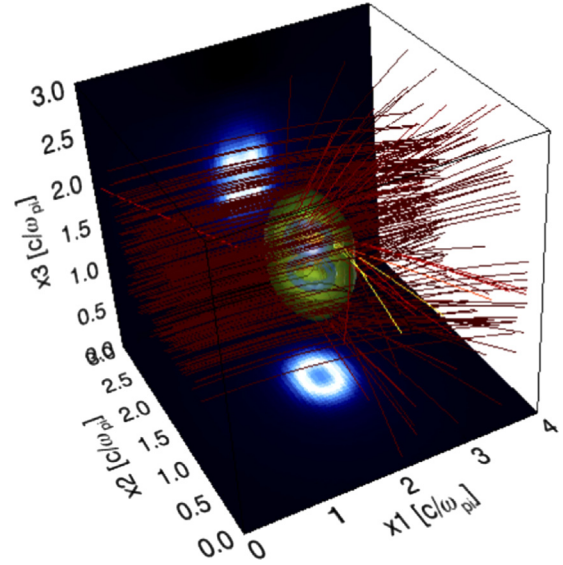

Fig. 7. A simulation of particle tracks (red) scattered from a thin electrostatic "shell" (green) surrounding a magnetic dipole (centre with *B* field intensity projected onto faces of the cube). The particles are not being deflected by the magnetic field but by the electric field resulting from the interaction of the background plasma (omitted for clarity) and the magnetic field. The energy of the red "protons" is 100,000 times that of the background plasma. Simulation is in dimensionless units. (For interpretation of the references to colour in this figure caption, the reader is referred to the web version of this paper.)

The geometry of this for our case is illustrated in Fig. 6.

In Cartesian coordinates, the deflection component of the electric field, $E_\perp$, required to narrowly miss the spacecraft, is acquired across the whole barrier width, L, in the one plane is $|E_\perp| = |E_r| \tan \theta$ where θ is the angle of the charged particle to the radial or the scattering angle.

The needed deflection velocity $v_\perp$ becomes:

$$v_\perp^2 \approx \frac{\kappa}{n_{mm}M} \frac{|\Delta B_{mm}^2|}{L} \tag{5.6}$$

As mentioned in Section 5.4, in 3D the physics is such that the electric field will always point outwards from the spacecraft. This results in a 3D safe zone effective against both directional and omni-directional threats. Thus we must determine the effectiveness of the high energy scattering process.

Because the electric field is formed self-consistently by the plasma itself, and the high energy particles are scattered by a lower electric field, the problem of generating a secondary population of ions accelerated towards the spacecraft by the deflector shield itself does not arise.

The mini-magnetosphere barrier interaction with high energy particles is far from simple. The incoming high energy particle not only encounters the electric field set up by the interaction of the solar wind and the spacecraft field, it also experiences the usual convective electric field as seen by a charged particle moving relative to a magnetic field. This convective field ($E_\perp$) is perpendicular to the magnetic field. As a result the particle is deflected by a series of fields in a complex manner [42].

Quantifying the shield performance for specific spectra of high energy particles (like an SEP) requires a full 3D recreation using a computer simulation, or an experiment, either in space or in the laboratory.

5.5.1. Computer simulation of high energy scattering

Fig. 7 shows a simulation of high energy scattering from a dipole magnetic field (centre of box). The 3000 "SEP" incoming ions are 100,000× the energy of the environmental ("solar wind") plasma within the box. The simulations show that 100% of the "SEP" particles were excluded from the "safe zone". For "SEP" particles approximately a million times the background energy, 95% of the particles were excluded. This indicates that a narrow electric field is responsible for the deflection rather than the gradual bending due to a magnetic field.

Additionally it indicates the high scattering efficiency of the high energy "SEP" ions by the sheath electric field formed by the background plasma.

5.6. Boosting the shield effectiveness: mass loading

The effects of the very largest storms could be mitigated by adding further plasma density around the spacecraft, similar to creating an artificial cometary halo cloud.

Increasing the density within the mini-magnetosphere reduces the thickness of the skin depth (Eq. (2)). This could be done either by reducing the power required from the space craft to achieve the same deflection efficiency, or by boosting the shield effectiveness during the most severe stages of an SEP or CME event.

Practically this could be done by releasing easily ionised material from the spacecraft. EUV ionisation, charge exchange, and collisional ionisation lead to the generation of ions and electrons which are incorporated in the mini-magnetosphere barrier. The mass loading leads to enhancement in the currents.

For manned spacecraft utilising Nuclear Thermal Propulsion (NTP) or Nuclear Electric Propulsion (NEP) as primary propulsion, this would already be achieved by the release of propellant from the thrusters; typical
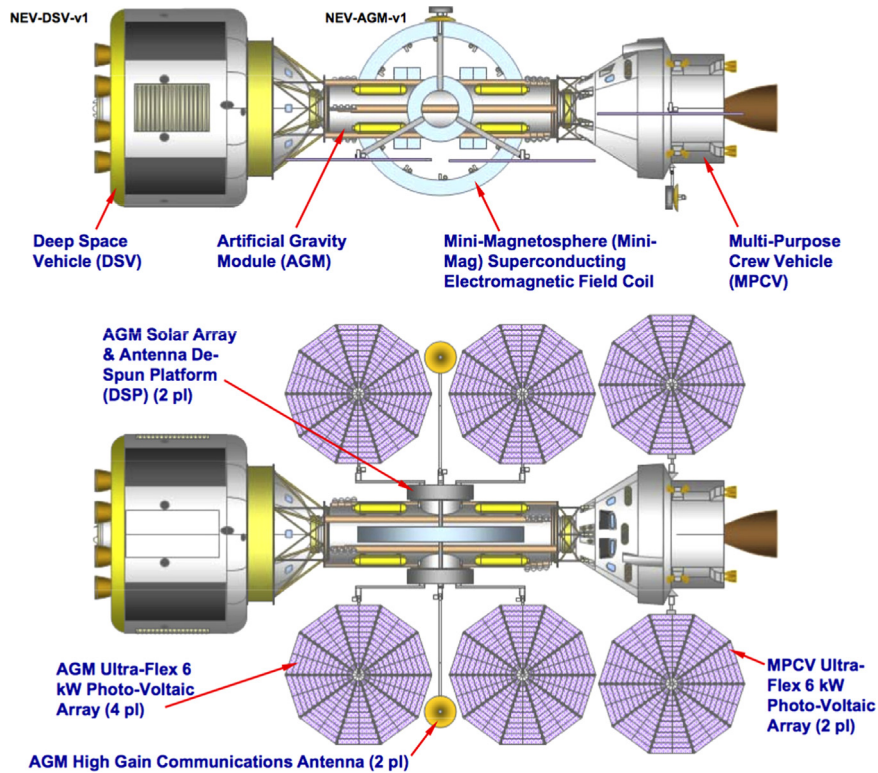
Fig. 8. A conceptual design for a manned interplanetary vehicle was presented by Benton [50] using current established technology and incorporated a mini-mag system.

propellants for these systems being hydrogen and other volatile propellants, while for NEP systems, inert gases such as argon and xenon could be used [45–47]. If more localised injection of plasma is required toward the shield region, ion or plasma sources, as already used for spacecraft propulsion [47], could provide more directed ion or plasma beams from multiple locations on the spacecraft. During the transit to Mars it might be necessary to use the augmented storm shield upon 0–2 occasions [8]. Increasing n_{mm} by $\times 10^4$ would provide an increase in the potential $\phi \sim \times 100$. This could be achieved by approximately 1 mole of Xe or Ar (in the volume of $\sim \frac{4}{3}\pi r_s^3$). Given that the atomic mass of Xe is ~ 131, for instance, this would mean 131 g of Xe would be needed per use.

Exactly how much Xe would be needed on a mission would depend upon the frequency of use. Allowing for approximately 3 SEP events to be encountered by the spacecraft in an 18 month period, this would require less than half a kilo of Xe.

It would also be necessary to sustain the enhancement for 2–6 h. The resources required would then depend upon the rate of plasma loss from the mini-magnetosphere. This is discussed in the next section.

5.7. Retaining the shield

To function as a shield, sufficient density must be retained for long enough within the cavity barrier to ensure the cavity is not overwhelmed by an intense storm for the duration of peak fluence (Fig. 3(a)). The plasma

parameter, β, defined as the ratio of the plasma pressure to the magnetic pressure, does not provide a useful guide in this instance because the profiles of plasma density and temperature vary on spacial scales below the ion gyration radius. Furthermore the parameter β does not allow for electric fields which we know are fundamental to the mini-magnetosphere barrier.

Since an analytical approach is not available as a guide, we can take an observational example from comets [51,23], and in particular the AMPTE artificial comet [24]. The data recorded by the spacecraft monitoring the active magnetospheric particle tracer explorers (AMPTE) mission, provide us with a lower limit of retention in the absence of a magnetic field. A ~ 1 kg mass of barium (amu=137) exhibits an ionisation time of ~ 20 min for a volume of 100 km^{-3} [48]. In the cometary case the particle pick-up means that the confinement structure is essentially open-ended and the matter is rapidly lost. The addition of a magnetic field would undoubtably extend the plasma retention (as is the case with magnetically confined plasma fusion experiments such as JET [53]) but to precisely what extent, particularly on the scale size of a mini-magnetosphere, could only be determined experimentally in space.

6. Estimating the requirements of the on board hardware

Having outlined the principles behind the mini-magnetosphere shield operation, and assembled some performance parameters, we can now compute some figures of merit.
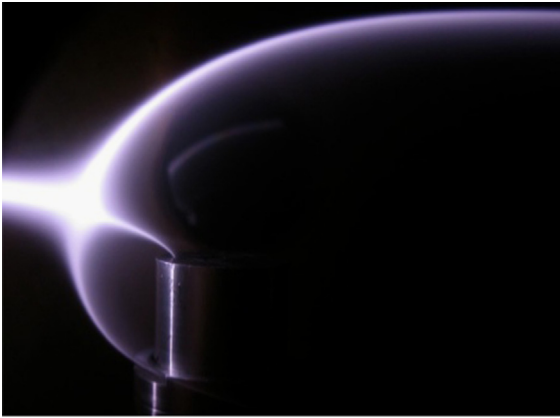
Fig. 9. A photograph of a mini-magnetosphere diamagnetic cavity formed in a laboratory Solar Wind Tunnel [21]. The "light" areas show where the plasma is present. The beam comes in from the left hand side and gets redirected into a thin layer around the target. The width of the layer L and the stand-off distance r_s agree very well with those expected by Eqs. (5.1) and (5.2).

A conceptual deep space vehicle for human exploration described in [22] included a mini-magnetosphere radiation shield. The purpose was to present a candidate vehicle concept to accomplish a potential manned near-Earth object asteroid exploration mission. The power (including cryo-plant), physical dimensions, magnetic field intensities and density augmentation capabilities used here will be those presented in [22,49].

For example, a maximum feasible coil radius of 3.0 m (set by a typical launch rocket fairing), $I_c = 700$ A, $N = 8000$ resulting from Eq. (4.1) in $NI_c = 5.6$ MAt. Inserting all the practical parameters provides $r_s = 0.86/P_{in}^{1/6}$ in units of km and nPa.

The total mini-magnetosphere power demand limit would be 16 kW, including 5 kW for the cryo-plant and the control system. The total mass was $\sim 1.53 \times 10^3$ kg including an estimated 250 kg of seed gas [22,49]. Fig. 8. shows how such a mini-magnetosphere system integrates with a spacecraft [50].

7. Evidence for the processes from other fields

The experimental and observational evidence in the formation of mini-magnetospheres has been established in the laboratory using Solar Wind Plasma Tunnels [21,38] and spacecraft observations of natural mini-magnetospheres on the Moon [16,39].

A photograph of a laboratory scale mini-magnetosphere is shown in Fig. 9 [21]. A vacuum or an MHD (magnetohydrodynamic) description of the laboratory experiment would have predicted that the plasma stream would not be deflected and would hit the magnet.

8. Summary

The equations provided above, can only give approximate values as the complexity of the interaction is highly variable, with multiple parameters inter-dependant in both time and orientation. This is a typical description of a non-linear system. We know that mini-magnetospheres work because of the example on the Moon [16,39]. We know that the same principles used here occur for both natural and artificial comets [51,26].

Injection of additional cold plasma from the spacecraft, such as xenon or krypton gas, which can easily be ionised by UV-radiation from the Sun, will significantly enhance the effectiveness of the shield.

The concept of placing a plasma around a spacecraft may at first sound familiar to those looking at active shield systems [36]. These, amongst others, have proposed various "Plasma Shield" schemes using flowing currents in plasmas around the spacecraft as means to extend the magnetic field or source of electrons to counter the incoming protons. The difficulty with these schemes has been omission of the role played by the environmental plasma, whose effect is to short circuit, screen or disperse the mini-magnetosphere plasma. The scheme suggested here does not attempt to control the plasma entirely but instead seeks to confine it sufficiently to allow its own nature to achieve the aim.

Regardless of whether some of the details contained herein, can be improved or adapted, this paper has aimed to emphasise the importance of including the plasma environment when considering any means of active or electromagnetic shielding to protect spacecraft from ionising radiation.

This paper has also aimed to demonstrate the importance of using the appropriate plasma physics dominant on the "human" rather than "celestial" scale.

To estimate a realistic prediction of effectiveness we have sought to provide approximate expressions which are credible and not to underplay the complexity of research needed.

The analysis shown here is for a modest powered mini-magnetosphere system which may function as a permanent means to increase the safe operating time for crew and systems in interplanetary space, functioning in much the same way as does the Earth's magnetosphere. Such a shield could also be enhanced to deal with extreme storms, against which it may be the only means of providing effective protection.

9. Conclusions

Proposals for electromagnetic shields generally come with highly optimistic predictions of effectiveness, yet no such prototype system has been tried in space, perhaps because of the lack of credibility of such claims.

This paper has presented an indication of the true complexity involved in active shielding.

Calculations which have assumed a vacuum are incorrect because in fact a plasma exists. The role of the plasma environment has either been overlooked completely, or it has been analysed on an inappropriate scale size.

Much detail has yet to be determined. An active shield system may not be practical without on-board power systems comparable to those envisioned in science fiction, but the concept should not be dismissed on the basis of an incorrect analysis.

An active deflector shield system could never replace passive shielding or biological advances, but it can offer options, particularly for EVAs, extending the longevity of hardware and preventing secondary activation of the ship's hull and systems. It seems the only credible theory for deflection of GeV particles.

The evidence that mini-magnetospheres actually work on the bulk plasma in space comes from magnetic anomalies on the moon [39,40], around asteroids [17] and comets, both natural [23] and artificial [48]. This, combined with laboratory experiments [25] and simulations, suggests that the high energy distribution can be sufficiently effected to justify optimism.

The value of being able to predict the occurrence of potentially lethal storms can only be fully realised if we can develop the means to provide safe shelter.

Acknowledgements

References

[1] International Space Exploration Coordination Group (ISECG), The Global Exploration Roadmap, 2013, see ⟨http://www.globalspaceexploration.org/web/isecg/news/2013-08-20⟩.

[2] P.D. Spudis, An argument for human exploration of the Moon and Mars, American Scientist 80 (1992) 269–277.

[3] I.A. Crawford, The scientific case for renewed human activities on the Moon, Space Policy 20 (2004) 91–97.

[4] P. Ehrenfreund, et al., Toward a global space exploration program: a stepping stone approach, Adv. Space Res. 49 (2012) 2–48.

[5] M. Lockwood, M. Hapgood, The rough guide to the Moon and Mars, Astron. Geophys. 48 (2007) 6.11–6.17.

[6] Committee on the Evaluation of Radiation Shielding for Space Exploration, National Research Council, Managing Space Radiation Risk in the New Era of Space Exploration, The National Academies Press, ISBN 9780309113830, 2008. ⟨http://www.nap.edu/openbook.php?record_id=12045⟩.

[7] F.A. Cucinotta, et al., Space radiation cancer risks and uncertainties for Mars missions, Radiat. Res. 156 (November (5)) (2001) 682–688.

[8] Myung Hee Y. Kim, et al., Prediction of frequency and exposure level of solar particle events, Health Phys. 97 (1) (2009) 68–81.

[9] F.A. Cucinotta, et al., Space radiation risk limits and Earth Moon Mars environmental models, Space Weather 8 (12) (2010).

[10] Francis A. Cucinotta, Marco Durante, Cancer risk from exposure to galactic cosmic rays: implications for space exploration by human beings, Lancet Oncol. 7 (5) (2006) 431–435.

[11] ⟨http://http://emmrem.unh.edu/⟩.

[12] J.H. Adams, Jr., et al., Revolutionary Concepts of Radiation Shielding for Human Exploration of Space, NASA TM 213688, 2005.

[13] Hannes Alfvén, Plasma in laboratory and space, J. Phys. Colloq. 40 (C7) (1979). C7-1.

[15] John Ashworth Ratcliffe, An Introduction to the Ionosphere and Magnetosphere, CUP Archive, 1972.

[16] R.P. Lin, et al., Lunar surface magnetic fields and their interaction with the solar wind: results from lunar prospector, Science 281 (1998) 1480.

[17] M.G. Kivelson, et al., Magnetic field signatures near Galileo's closest approach to Gaspra, Science—N. Y. Wash. 261 (1993) 331.

[18] J.S. Halekas, et al., Density cavity observed over a strong lunar crustal magnetic anomaly in the solar wind: a mini-magnetosphere? Planet. Space Sci. 56 (7) (2008) 941–946.

[19] L.L. Hood, C.R. Williams, The lunar swirls—distribution and possible origins, in: Lunar and Planetary Science Conference Proceedings, vol. 19, 1989.

[20] B.J. Anderson, et al., The global magnetic eld of Mercury from MESSENGER orbital observations, Science 333 (605) (2011) 1859–1862.

[21] R. Bamford, et al., The interaction of a flowing plasma with a dipole magnetic field: measurements and modelling of a diamagnetic cavity relevant to spacecraft protection, Plasma Phys. Control. Fusion 50 (12) (2008) 124025.

[22] M.G. Benton Sr., et al., Concept for human exploration of NEO asteroids using MPCV, deep space vehicle, artificial gravity module, and mini-magnetosphere radiation shield, in: 44th AIAA SPACE 2011 Conference and Exposition, AIAA-2011-7138, Long Beach, CA, 2011.

[23] A.J. Coates, et al., Plasma parameters near the comet Halley bow shock, J. Geophys. Res.: Space Phys. (1978–2012) 95 (A12) (1990) 20701–20716.

[24] D.A. Bryant, S.M. Krimigis, G. Haerendel, Outline of the active magnetospheric particle tracer explorers (AMPTE) mission, IEEE Trans. Geosci. Remote Sens. 3 (1985) 177–181.

[25] P. Muggli, et al., Collective refraction of a beam of electrons at a plasma–gas interface, Phys. Rev. Spec. Top.—Accel. Beams 4 (9) (2001) 091301.

[26] R. Bingham, et al., Theory of wave activity occurring in the AMPTE artificial comet, Phys. Fluids B: Plasma Phys. 3 (1991) 1728.

[28] H.V. Cane, D.V. Reames, T.T. Rosenvinge, The role of interplanetary shocks in the longitude distribution of solar energetic particles (1978–2012), J. Geophys. Res.: Space Phys. 93 (A9) (1988) 9555–9567.

[29] K.G. McClements, et al., Acceleration of cosmic ray electrons by ion-excited waves at quasiperpendicular shocks, Mon. Not. R. Astron. Soc. 291 (1) (1997) 241–249.

[30] R.A. Mewaldt, et al., Solar-particle energy spectra during the large events of October–November 2003 and January 2005, in: 29th International Cosmic Ray Conference, Pune, 2005, pp. 101–104.

[31] L.W. Townsend, Implications of the space radiation environment for human exploration in deep space, Radiat. Prot. Dosim. 115 (1–4) (2005) 44–50.

[32] Honglu Wu, et al., Risk of Acute Radiation Syndromes Due to Solar Particle Events, H NASA, HHC, 2008.

[33] Thomas B. Borak, Lawrence H. Heilbronn, Lawrence W. Townsend, Rafe A. McBeth, Wouter de Wet, Quality factors for space radiation: a new approach, Life Sci. Space Res., Available online 17 February 2014, ISSN 2214-5524, http://dx.doi.org/10.1016/j.lssr.2014.02.005.

[34] Eugene N. Parker, Shielding space travelers, Sci. Am. 294 (3) (2006) 40–47.

[36] F.W. French, R.H. Levy, Plasma radiation shield—concept and applications to space vehicles, J. Spacecr. Rockets 5 (5) (1968) 570–577.

[38] L. Gargaté, et al., Hybrid simulations of mini-magnetospheres in the laboratory, Plasma Phys. Control. Fusion 50 (7) (2008) 074017.

[39] R.A. Bamford, et al., Mini-magnetospheres above the lunar surface and the formation of lunar swirls, Phys. Rev. Lett. 109 (2012) 081101.

[40] R.A. Bamford, et al., PIC code simulations mini-magnetospheres above the lunar surface, in preparation, 2014.

[41] D. Tidman, N.A. Krall, Shock Waves in Collisionless Plasmas, S.C. Brown (Ed.), John Wiley and Sons, New York, 1971.

[42] L.C. Woods, Principles of Magnetoplasmas, Clarendon, Oxford, 1987, p. 397.

[43] A.D.R. Phelps, Interactions of plasmas with magnetic field boundaries, Planet. Space Sci. 21 (9) (1973) 1497–1509.

[45] U. Guyen, Nuclear Propulsion Techniques for Spacecraft: Utilization of Nuclear Reactors in Spacecraft for Space Propulsion and Space Power in a Microgravity Environment, LAP Lambert Academic Publishing, 2011.

[46] K.F. Long, Deep Space Propulsion, Springer, 2012.

[47] D. Goebel, I. Katz, Fundamentals of Electric Propulsion, Wiley-Blackwell, London, 2008.

[48] H. Lühr, et al., in situ magnetic field observations of the AMPTE artificial comet, Nature 320 (1986) 708–711.

[49] Mark G. Benton Sr. et al., Modular space vehicle architecture for human exploration of mars using artificial gravity and mini-magnetosphere crew radiation shield, in: 50th AIAA Aerospace Sciences Meeting and Aerospace Exposition, AIAA-2012-0633, Nashville, TN, 2012.

[50] Mark G. Benton Sr., Conceptual common modular design for crew and cargo landers and deep space vehicles for human exploration of the solar system, in: AIAA Space 2013 Conference, AIAA-2013-5355, San Diego, CA, 2013.

[51] A.A. Galeev, Solar wind interaction with comet Halley, Adv. Space Res. 5 (12) (1985) 155–163.

[53] ⟨http://www.efda.org/jet/⟩.